ELSEVIER

Neurobiology of Aging 22 (2001) 737–745

NEUROBIOLOGY OF AGING

www.elsevier.com/locate/neuaging

MRI of human entorhinal cortex: a reliable protocol for volumetric measurement

I.I. Goncharova[a,1], B.C. Dickerson[a,2], T. R. Stoub[a], L. deToledo-Morrell[a,b,c,*]

[a]*Department of Neurological Sciences, Rush University, 1653 W. Congress Parkway, Chicago, IL 60612, USA*
[b]*Rush Alzheimer's Disease Center, Rush University, Chicago, IL 60612, USA*
[c]*Department of Psychology, Rush University, Chicago, IL 60612, USA*

Received 15 July 2000; received in revised form 20 June 2001; accepted 20 June 2001

Abstract

A new protocol for measuring the volume of the entorhinal cortex (EC) from magnetic resonance images (MRI) was developed specifically to measure the EC from oblique coronal sections used in hippocampal volumetric studies. The relative positions of the anatomic landmarks demarcating EC boundaries were transposed from standard coronal sections to oblique ones. The lateral EC border, which is the most controversial among anatomists, was defined in a standard and conservative manner at the medial edge of the collateral sulcus. Two raters measured the EC twice for 78 subjects (healthy aged individuals, very mild AD patients, and elderly patients who did not meet criteria for dementia) to study intra- and inter-rater reproducibility and reliability of measurements. The level of accuracy achieved (coefficients of reproducibility of 1.40–3.86%) and reliability of measurements (intraclass correlation coefficients of 0.959–0.997) indicated that this method provides a feasible tool for measuring the volume of the EC in vivo. © 2001 Elsevier Science Inc. All rights reserved.

Keywords: Hippocampal formation; Imaging; Parahippocampal gyrus; Aging; Alzheimer's disease; Reliability study

1. Introduction

The entorhinal cortex (EC), which connects the hippocampal formation (HF) with neocortical regions and supplies it with multimodal information, is considered to be a critical component of the mesial temporal lobe memory system [48,49,53,54]. While the HF has received a great deal of attention in magnetic resonance imaging (MRI) studies of the anatomic pathology that occurs in Alzheimer's disease (AD) [9,11–13,29,30,33–35,39,41,44], the EC had not been studied using quantitative MRI methods until recently [4,24,27,36,52]. However, a number of post-mortem histopathological studies based on neuronal counts, as well as the distribution of neurofibrillary tangles, neuropil threads, and senile plaques, have documented the involvement of the EC early in the course of AD [5,7,21,25, 51]. Compared to the EC, the HF of patients dying with relatively mild dementia contains significant, but somewhat less pathology [2,5,7,10,21,25,42]. These data suggest that in vivo EC measurements may have the potential to identify anatomic changes in the earliest stages of AD.

Entorhinal atrophy in vivo in AD patients was initially detected by semi-quantitative visual rating of MR images [14,20,43]. Partly due to the fact that the rostral EC boundaries with adjacent structures (primary olfactory cortex, perirhinal cortex) are not demarcated macroscopically, some investigators [3,14,36,45] measured EC volume using only one to three sections from the mid-portion of the structure, where those problematic boundaries are not present. The majority of these studies [3,14,45] demonstrated equivalent atrophy of the EC and of the HF in patients with mild to moderate dementia. Using a measure of the EC surface area, Bobinski et al. [4] reported good discrimination between mild AD patients and healthy aged subjects. It was only recently that protocols were published to measure the entire volume of the EC from MR images [24,27]; Insausti et al. [27] validated their protocol using

* Corresponding author. Tel.: +1-(312) 942-5399; fax: +1-(312) 942-2238.

E-mail address: ldetoled@rush.edu (L. de Toledo-Morrell).

[1]Present address: Wadsworth Center, New York State Department of Health, Albany, NY.

[2]Present address: Departments of Neurology, Massachusetts General and Brigham and Women's Hospitals, Harvard Medical School, Boston, MA. This research was supported by grants P01 AG09466 and P30 AG10161 from the National Institute on Aging, National Institutes of Health.

0197-4580/01/$ – see front matter © 2001 Elsevier Science Inc. All rights reserved.
PII: S0197-4580(01)00270-6

cytoarchitectonic material. Studies based on the latter protocol have demonstrated an absence of age-related changes in the EC when young and aged control subjects were compared [27], extensive atrophy (40%) in AD patients, and a high level of statistical power in discriminating AD patients from healthy aged individuals [31,32]. Still, two methodological problems regarding the volumetric measurement of the EC remain.

Published quantitative protocols for volumetry of the entire EC [24,27] were developed for coronal sections oriented perpendicularly to the line connecting the anterior and posterior commissures (AC-PC), since the borders of the EC have been described histologically using standard anatomic dissections [1,6,27,28,38,49,50]. However, in many laboratories the HF is measured from coronal sections oriented perpendicularly to its long axis, and it is important to measure the EC from the same oblique coronal sections to avoid overestimation of the volume of one of these two adjacent structures at the expense of the other. Therefore, we conducted a pilot study to transpose the relative positions of the anatomic landmarks demarcating EC boundaries from the standard coronal plane to the oblique coronal plane.

The other problem is related to the lateral boundary of the EC, which is not uniformly defined cytoarchitectonically because of individual differences [28,38]. Some anatomists locate the lateral border at varying points along the medial bank of the collateral sulcus (CS) and consider it as the entorhinal/perirhinal border [1,28], while others locate it at the medial edge of the CS [49,50], and consider it as the entorhinal/transentorhinal border [6,8,23]. The published protocols for EC measurement differ in definitions of the lateral border, either locating it at the fundus of the CS [4,24] or constructing it at some point along the CS depending on its length [27]. This controversy reflects different approaches to real anatomic variations between individuals. In the work described herein, the lateral border of the EC was defined in a conservative and standard manner, at the medial edge of the CS for all cases.

In this study, a protocol for measuring the volume of the EC from consecutive oblique coronal sections was developed in order to compare disease-induced changes in the EC and HF. Images obtained from healthy aged subjects, patients with very mild AD and elderly patients who did not meet diagnostic criteria for dementia were used in this work. The protocol for EC measurement is described in detail in this paper, while data comparing the three groups of subjects are reported in the accompanying paper [15].

2. Methods

2.1. Subjects

The data reported here were obtained from three groups of participants, consisting of a) 34 healthy elderly individuals, b) 28 elderly patients who presented at the clinic with cognitive complaints but did not meet criteria for dementia, and c) 16 patients with a clinical diagnosis of very mild probable AD [see selection criteria in the accompanying paper, [15]]. A group of 10 healthy young subjects (mean age = 28.5, range = 22–32 years) participated in the pilot study conducted to test the effects of slice orientation on EC boundary definitions. Informed consent was obtained from all participants according to the guidelines of the Institutional Review Board of Rush Medical College.

2.2. Acquisition of MR image data

MR images were acquired on a 1.5 T imaging system (Signa, General Electric Medical Systems, Milwaukee, WI). Gapless, 5 mm coronal slices were taken perpendicular to the long axis of the hippocampal formation using the following parameters: matrix = 256 × 256, field of view = 16 cm, eight acquisitions, TRH = 400, TE = 13–16. In addition, gapless 5 mm sagittal slices were taken spanning the entire brain with the following parameters: matrix = 256 × 128, field of view = 24 cm, one acquisition, TRH = 200, TE = 12.

Our MRI acquisition protocol has changed since the initiation of this study. In order to have large enough sample sizes in the various groups and for purposes of consistency, the analysis of reliability of measurements in this study was restricted to those elderly subjects scanned with the old MRI acquisition protocol. In the pilot study, images were acquired using the scanner manufacturer's 3D Fourier transform spoiled gradient recalled (SPGR) pulse sequence with the following parameters: 124 contiguous images were acquired in the coronal plane, 1.6 mm thick, matrix = 256 × 192, field of view = 22 cm, TR/TE = 33.3/7 msec, flip angle = 45 degrees, signals averaged = 1.

2.3. Image processing

Manual tracing of structures and volume computations were performed using the Amersham Image Analysis System (with software designed by Loats Associates, Westminster, MD), running on a PC-compatible computer.

In the pilot study, the effects of slice orientation on EC boundary definitions were tested using the multiplanar reformatting procedures of the $\text{Analyze}_{\text{AVW}}$ software package (Mayo Foundation, Rochester, MN). In this part of the study, to increase the accuracy of transposing from one orientation to the other, slices initially acquired at a thickness of 1.6 mm were resliced as 0.5 mm sections.

2.4. Protocol development

The protocol for outlining the EC was developed using published anatomic atlases [17,18], morphological and cytoarchitectonic studies [1,6,22,27,28,38,49,50], as well as advice from Dr. G. W. Van Hoesen (personal communication).

Topographical relations between anatomic landmarks

and microscopically defined EC borders are given in the literature for standard anatomic dissections, which correspond to MR sections oriented perpendicularly to the AC-PC line at the midsagittal level. To define EC borders in the oblique plane used in HF volumetry (i.e. oriented perpendicularly to the long axis of the HF), we compared the relative positions of known anatomic landmarks in the two planes. Images of the same brain were resliced in both orientations. The rostral limit of the temporal horn of the lateral ventricle was taken as a reference point (zero level). The two sets of images from the same brain were aligned by this zero level, and the relative distances between the anatomic landmarks were calculated from resized 0.5 mm-thick sections.

2.5. Reliability and accuracy of EC measurement

Two raters (IG and BD), blinded to clinical data and diagnoses, examined images together, and came to an agreement on the identification of sulci demarcating the boundaries of the EC for each subject. Then, the raters worked independently to outline the EC using the protocol described below. They each measured the left and the right EC twice for all the subjects under study. The accuracy of measurement (intra- and inter-rater reproducibility) and coefficients of reliability were calculated separately for the left and right hemispheres in each of the three groups of elderly participants. In addition, one rater measured the EC twice from all the individual images using the lateral EC border criterion of Insausti et al. [27].

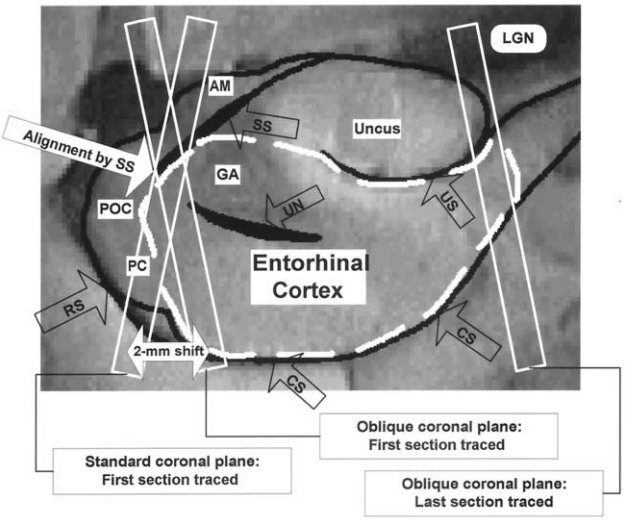

Fig. 1. A diagram of the parahippocampal gyrus in sagittal view showing the borders of the EC, bordering structures, MRI sections in standard and oblique planes, and relative positions of conspicuous landmarks used for tracing the EC. Anatomic structures bordering the EC are: AM-amygdala; GA-gyrus ambiens; LGN-lateral geniculate nucleus; PC-perirhinal cortex; POC-primary olfactory cortex. The uncus is included within the HF. The main gyri are indicated by black arrows: CS-collateral sulcus; RS-rhinal sulcus; SS-sulcus semianularis; UN-uncal notch; US-uncal sulcus. See text for details concerning alignment of in the two planes and first and last images traced.

3. Results

3.1. Effects of slice orientation (pilot study)

The effects of slice orientation on EC boundaries are demonstrated in Fig. 1.

In the standard AC-PC plane, the rostral limit of the EC is located approximately 2 mm posterior to the level of the temporal stem (limen insulae; 1,27,28). In oblique coronal sections, the temporal stem appears, on average, 4.2 mm posterior to that in standard coronal sections in the left hemisphere (range: 3–5.5 mm) and 4.3 mm posterior in the right (range: 2–7 mm). Consequently, due to rotation, the rostral limit of the EC should be located approximately 2 mm *anterior* to the temporal stem in the oblique plane.

An important effect of slice orientation was found in the appearance of the EC in the first MRI section traced. In the standard plane, the first section used for tracing included the EC superiorly and perirhinal cortex inferiorly, with an indiscernible border between the two regions (see Fig. 1, “Standard coronal plane: First section traced”). In the protocol developed by Insausti et al. [27], this border was approximated by subdividing the medial aspect of the parahippocampal gyrus (PHG) into two halves, with the superomedial one belonging to the EC. In the present study, when the first appearance of the sulcus semianularis (which marks the superior EC-amygdala border, 17,49) in the oblique plane was aligned with the same point in the standard plane (Fig. 1, arrow showing alignment by SS), the oblique section was shifted posteriorly by 2 mm along the inferior aspect of the PHG (see double headed arrow in Fig 1). Because of this shift, the inferior aspect of the first oblique section corresponded to that of the second standard section, where the inferior portion of the PHG was considered to be occupied solely by the EC [27]. Thus, by starting to measure at this level in the oblique plane, the indiscernible entorhinal/perirhinal border was avoided; however, the very rostral tip of the EC was probably excluded in our protocol.

The lateral geniculate nucleus (LGN) was used as the caudal limit of the EC [1,6]. In oblique sections, it was seen, on average, 1.5 mm posterior to its appearance in standard sections. Therefore, if 5 mm thick images are used, the section preceding that where the LGN is first seen would be the last one containing the EC. This section was the last one in which the uncus was visible (see Fig 1., “Oblique coronal plane: Last section traced”). It should be noted that in the histology-based protocol of Insausti et al. [27], the slice in which the uncus (the gyrus intralimbicus) was still visible, was also the last one in which the EC was traced.

The relative positions of anatomic landmarks as they appeared in oblique coronal sections were used to define the EC boundaries, which are described below.

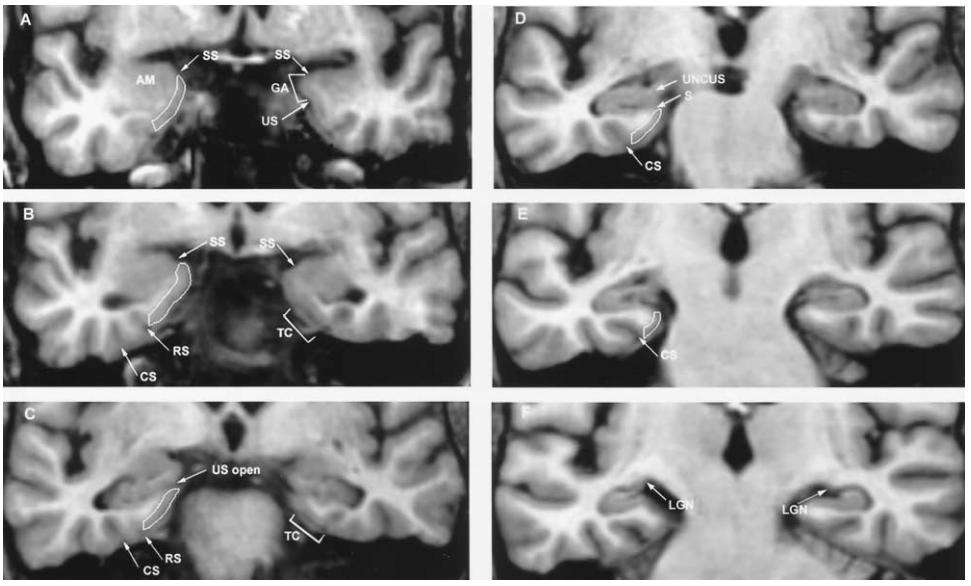

Fig. 2. Outline of the right entorhinal cortex (EC) on oblique coronal sections (A-E). On the first section in which the EC is outlined (A), the gyrus ambiens (GA), amygdala (AM) and white matter of the parahippocampal gyrus (PHG) are formed. The temporal stem (limen insulae) is visible on both sides. Outline of the right EC (left hand-side of each section) includes the gyrus ambiens (GA) starting from the fundus of the sulcus semianularis (SS) and cortical gray matter, along the medial aspect of the PHG down to the medial edge of the lateral branch of the rhinal sulcus (RS) in the first three sections (A- C). In sections D and E, tracing was stopped at the medial edge of the collateral sulcus (CS), since the RS was no longer present. On the second section (B), where a portion of the hippocampal formation (HF) is present, the "inner" border is outlined by the gray/white matter interface, then up to the SS, excluding the HF. The uncal sulcus (US) is open on posterior sections (marked on C). Starting from the level at C, the GA is no longer present, but is replaced by the uncus of the HF. Supero-medially the EC borders the subiculum. This border is traced from the apex of the PHG (C and D), or from the most medial point of the PHG (excluding the subiculum) on the last section (E), in which the uncus is still visible. The tentorium cerebelli (TC) is in close proximity to the "outer" border of the EC (marked on the left temporal lobe, sections B and C, right-hand side of the figure). The lateral geniculate nucleus (LGN) is shown in section F.

3.2. Entorhinal cortex: boundary definitions

Outlines of the EC on consecutive coronal sections taken perpendicular to the long axis of the HF are shown in Fig. 2.

The rostral limit of the EC was defined as the level where the gyrus ambiens (Brodmann's area 34 representing the supero-medial portion of the EC; 17, 50), amygdala, and white matter of the PHG are first visible. In this section, which was the first one traced (Fig. 2A), the sulcus semianularis and the temporal stem could also be seen.

The caudal limit of the EC was defined by the first appearance of the LGN (Fig. 2F). The image immediately preceding the one with the LGN was the last section traced. In this section (Fig. 2 E), the uncus was visible.

The sulcus semianularis, which separates the gyrus ambiens from the amygdala [17,49], defined the supero-medial limit of the EC (see Figs. 2A and B, left hemisphere). It was clearly visible in most cases in the first section where the EC was traced. In more caudal sections, the gyrus ambiens is no longer present; instead, the uncus of the HF appears at this level (Fig. 2 C-E). The uncal sulcus is a conspicuous landmark that demarcates this transition [17,49,50]. Starting from the section in which the uncal sulcus was discernible and could be followed without interruption from its fundus all the way out to the medial surface (i.e. the sulcus was "open," Fig. 2 C-E), all the tissue superior to the sulcus was considered to belong to the HF. Therefore, the supero-medial border of the EC was defined by the inferior border of the subiculum.

Infero-laterally, the EC is limited by the lateral branch of the rhinal sulcus or collateral sulcus. Only one of the two is usually present on a particular section. If both sulci or the two parts of the interrupted collateral sulcus were present on the same section, the one most medially located was used as the infero-lateral limit of the EC. This case is illustrated in Fig. 2 (A and B, right temporal lobe, and C, left temporal lobe).

As it follows from the cytoarchitectonic studies cited in the introduction, the lateral border of the EC is the most variable among individuals, and its location is the most controversial among authors. We defined the lateral border of the EC as the most infero-medial point of the medial bank of the collateral sulcus for all cases, i.e. at the point of the sharpest curvature of the edge of the PHG as it turns into this sulcus.

3.3. Tracing of the EC

The EC was traced in a rostral-to-caudal direction. On sections crossing the gyrus ambiens (Fig. 2 A-B), the EC was outlined supero-medially by tracing the contour of the gyrus ambiens beginning from the fundus of the sulcus semianularis, and downward along the medial aspect of the PHG following the tissue-CSF interface. The tracing of this

"outer" border was stopped at the medial edge of the collateral (or rhinal) sulcus. The lateral border of the EC was constructed as a line perpendicular to the surface of the PHG starting at the medial edge of the sulcus. The "inner" border was traced along the PHG gray/white matter interface, which is usually clearly visible up to the level of the uncal notch. The rest of the "inner" border was then interpolated by drawing a straight line to the fundus of the sulcus semiannularis (excluding the HF, if present; see Fig. 2 B).

In caudal sections, starting from the one where the uncal sulcus is open (Fig. 2 C), the EC was outlined superomedially at the subiculum/entorhinal border. If not evident, the border was constructed by drawing a line connecting the most medial point of the PHG with the most medial point of the white matter of the PHG (Fig. 2 C-E). The other borders were outlined in the same manner as in rostral sections.

This protocol for outlining the EC differed from previously published ones [24,27] in slice orientation (which mostly affected the first section traced), and in the definition of the lateral EC boundary. While Honeycutt et al. [24] defined the lateral EC border at the fundus of the collateral sulcus, Insausti et al. [27] located this border differently in the following cases: at the medial edge of the collateral sulcus if it was deep (more than 1.5 mm), at the midpoint of the sulcus if it was regular (1 to 1.5 mm) and at the fundus of the sulcus if it was shallow [27]. Methodologically, our criterion for outlining the lateral EC border was less time consuming and more conservative. However, it probably left out a small portion of the EC, at least in some cases. Since the lateral border definition used by Insausti and colleagues [27] was based on histologic material, and because of the evidence from histopathological studies indicating that the area situated along the collateral sulcus may be among the earliest sites of degeneration in AD [6,7], we decided to reproduce their method along with ours, and to compare the two empirically.

3.4. Comparison of two methods for outlining the lateral EC border

Fig. 3 presents distributions of EC volumes for the three groups under study, obtained using two different methods for defining the lateral EC boundary: with the lateral border limited to the medial edge of the collateral sulcus and with the lateral border located at some point along its medial bank, depending on its depth [27]. Volumes of the EC were higher for the second method. To make the data comparable, absolute EC volumes (the mean of the two measurements obtained by the same rater) were transformed to Z-scores. As can be seen in Fig. 3, the distributions obtained by the two methods were extremely similar. The similarity of the two distributions was confirmed by a high correlation between the data obtained by the two methods across all the subjects (Pearson's $r = 0.924$, $P < 0.0005$, $N = 78$).

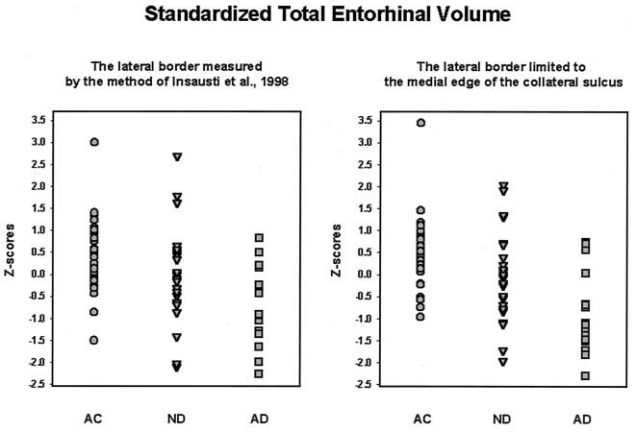

Fig. 3. Distribution of standardized EC volumes in the three groups of subjects, obtained by two different methods of measurement: A - with the lateral EC border as measured by Insausti and colleagues [27], and B - with the lateral EC border limited to the medial edge of the collateral sulcus. AC denotes the aged control group, ND the non-demented group and AD, patients with Alzheimer's disease.

3.5. Reproducibility of measurements

In the subjects included in the present study, the number of sections taken for EC measurement varied from 4 to 6; the average number of sections was 4.67 for the left and 4.70 for the right hemisphere. The rostral-to-caudal length of the structure was found to be, on average, 23.35 mm for the left EC and 23.50 mm for the right. These values were close to those (22.6 mm and 23.8 mm, respectively) reported by Insausti et al. [27]. Absolute EC volumes for the three groups of elderly participants are shown in Table 1, together with standard deviations and coefficients of variation. As can be seen from this table, EC volumes showed high individual variability, as assessed by coefficients of variation, a measure that allows comparison of individual differences in subsets of data irrespective of their mean values.

Table 1
Mean absolute entorhinal cortex volumes in mm^3

Group		Left EC	Right EC
Aged controls (N = 34)	Mean	779.08	811.29
	SD	156.94	156.38
	CV%	20.14	19.28
Non-demented (N = 28)	Mean	648.99	719.21
	SD	165.31	216.69
	CV%	25.47	30.13
Mild AD (N = 16)	Mean	517.73	553.98
	SD	188.41	179.88
	CV%	36.39	32.47

Means of volumes (mm^3), standard deviations (SD) and coefficients of variation (CV%), are based on the average of four measurements obtained by the two raters. Coefficients of variation are calculated as a percentage of the standard deviation of individual EC volumes from their mean values (see text).

Table 2
Reproducibility of EC measurements

Group	Intra-rater data (B.D.)		Intra-rater data (I.G.)		Inter-rater data	
	Left EC	Right EC	Left EC	Right EC	Left EC	Right EC
AC (N = 34)	1.61	1.69	1.65	2.16	2.79	2.24
ND (N = 28)	2.62	1.50	1.86	1.40	3.86	2.11
AD (N = 16)	3.51	2.13	2.85	2.48	3.37	3.46

Coefficients of reproducibility were calculated as a percentage of the standard deviation of differences between repeated measurements from the mean value of the same measurements (see text).

Results on reproducibility of measurements are shown in Table 2. Coefficients of intra-rater reproducibility were calculated as a percentage of the standard deviation of differences in repeated measurements obtained by one rater from the mean volume of the structure obtained by the same rater. Inter-rater reproducibility was calculated in the same manner; for each rater the first and second measurements were averaged. As can be seen from Table 2, the two raters were equivalently accurate on measurements.

3.6. Reliability of measurements

Reliability of measurements was assessed by the intra-class correlation method developed by Shrout and Fleiss [46, model 3], and modified for an experimental design where each of the fixed raters (i.e. the particular two raters, not any two from a population of raters) make repeated measurements on each subject [19]. This modification corresponds to the design of our study and has the advantage of giving concurrent assessment and comparable values for both measures of reliability, since both sources of error (inter-rater and intra-rater) are derived from the same statistical analysis.

The reliability coefficients and 95% one-sided lower-limit confidence intervals calculated for this modification of the analysis [19] are presented in Table 3. Statistical criteria developed for reliability studies give a number of critical values for testing estimated coefficients of reliability. Values of coefficients that fall in the interval 0.81–1.00 are considered as "almost perfect" and acceptable for other data analyses that require, at least, a 5% level of significance with 80% statistical power [16,19,40]. All 95% lower-limit confidence intervals estimated in our study exceeded the minimum level of "almost perfect" reliability (0.81). The null hypothesis (i.e. that our coefficients are not almost perfect) was tested against the critical value of 0.81 and rejected both for inter-rater and intra-rater coefficients of reliability ($P < 0.001$). Thus, it can be concluded that our EC measurements are better than "almost perfect."

In addition to coefficients of reliability assessed for each group of subjects, the group x rater residual error was estimated across all participants using the split-plot design. Three separate analyses (two-way repeated measures ANOVA with rater as within-subject and groups as between-subject factors) were performed on 1) the first measurements of each rater, 2) the second measurements, and 3) the average of the two measurements obtained by each rater. The analysis using the second measurements obtained by each rater gave the lowest group x rater residual error ($F(2,75) = 1.92$, $P = 0.153$ for the left EC, and $F(2,75) = 0.78$, $P = 0.461$ for the right EC), indicating that they were more reliable in describing the group data. Therefore, we

Table 3
Reliability of EC measurements

	Intra-rater data (B.D.)		Intra-rater data (I.G.)		Inter-rater data	
	Left EC	Right EC	Left EC	Right EC	Left EC	Right EC
Aged Controls						
Coefficient of reliability	0.989	0.990	0.991	0.984	0.959	0.972
(95% confidence intervals)	(0.981, 1)	(0.982, 1)	(0.984, 1)	(0.972, 1)	(0.934, 1)	(0.955, 1)
F (33,33); $p < 0.001$	19.97	21.20	23.52	13.07	7.43	11.43
Non-Demented						
Coefficient of reliability	0.986	0.995	0.994	0.997	0.963	0.984
(95% confidence intervals)	(0.984, 1)	(0.989, 1)	(0.988, 1)	(0.994, 1)	(0.938, 1)	(0.973, 1)
F (27,27); $p < 0.001$	14.78	38.75	34.98	65.68	8.12	19.44
Mild AD						
Coefficient of reliability	0.985	0.993	0.991	0.992	0.985	0.979
(95% confidence intervals)	(0.965, 1)	(0.984, 1)	(0.979, 1)	(0.983, 1)	(0.971, 1)	(0.958, 1)
F (15,15); $p < 0.001$	13.87	30.76	23.80	29.80	25.06	14.49

Coefficients of reliability were tested against 0.81, which is the lower limit for "almost perfect" reliability [20].

used the average of the second measurements obtained by each of the two raters in all analyses that compare EC volumes in the three group of subjects [see Dickerson et al. [15], accompanying paper].

4. Discussion

Many authors have emphasized that MRI volumetric methods are of the greatest clinical value if they are applied to patients with AD of mild severity [12,30] or to non-demented individuals "at risk for AD" [9,11,33,44,47,52]. However, the practical possibility of such studies is limited by the methodology of MRI volumetry; subtle early or pre-clinical changes in volumes can be detected only in brain structures that are amenable to accurate and reliable measurement. These methods have been well elaborated for the HF [e.g. 12,26,29,30,35], PHG [e.g. 12,30,34,37], and amygdala [e.g. 30, 35]. However, such methods are only beginning to be described for the EC.

In this paper, we present a method for reliably measuring the EC in vivo from MRI scans. The EC boundaries (except for the gray/white and the tissue/CSF interfaces) are not demarcated macroscopically. However, the medial temporal region has abundant conspicuous surface landmarks associated in their topography with cytoarchitectonically defined EC boundaries [22,27,28,49], which may be used for demarcating the EC from MR images. These landmarks are described in the literature for standard anatomic dissections taken perpendicularly to the line connecting the anterior and posterior commissures. In this study, we transferred the relative positions of these landmarks to the plane used in HF volumetry, i.e. image slices oriented perpendicularly to the long axis of the HF. By doing so, we developed a protocol for EC measurement that allows volumetry to be performed on both structures in the same plane. This is the main difference of our volumetric protocol from those previously described [24,27]. As a consequence of the difference in slice orientation, this protocol also differed in definitions of the rostral and caudal limits of the EC. However, results obtained with our protocol in terms of the rostral-to-caudal length of the structure were similar to data reported previously [27].

By defining the supero-medial border of the EC to include the gyrus ambiens, our protocol was similar to that of Insausti et al. [27], but different from that of Honeycutt and colleagues [24]. This area (Brodmann's area 34) belongs to the EC by histologic evidence [17,49,50]. It can be easily distinguished in the first EC section from the infero-medial portion of the amygdala using the sulcus semianularis as a landmark, and, in more caudal sections, from the pes hippocampi by the alveus. In the oblique coronal slice orientation, according to our estimation, the EC occupies the entire medial aspect of the PHG down to the collateral sulcus. Thus, orientation of sections perpendicular to the long axis of the HF removes the necessity to approximate the entorhinal/perirhinal border arbitrarily in the first section. This position of the first oblique section evidently excluded the most rostral tip of the EC, where its inferior border with the perirhinal cortex and, possibly, its superior border with the primary olfactory cortex cannot be determined from MR images.

Another difference between our protocol and those published previously [24,27] was in the definition of the lateral EC border. In our protocol, the lateral EC boundary was located at the medial edge of the collateral sulcus; it did not include the transentorhinal area [as defined by [6,8]] and avoided possible inclusion of the adjacent perirhinal cortex in some cases [27,28]. This way of outlining the EC avoided an additional source of possible operator error in measuring (or visually estimating) the length of the collateral sulcus and implementing differential criteria for the location of the lateral border, depending on the depth of the sulcus. However, we realize that our protocol may exclude the most lateral portion of the EC in some individuals. According to histopathological studies, the cortical area along the collateral sulcus is one of the sites where AD-related pathology is detected earliest [5,7,51]; therefore, it is of particular interest for in vivo MRI studies. However, in a cross-sectional study, this area introduces to volumetric values additional individual variability due to individual differences in the length of the collateral sulcus. This additional variability may be unequally distributed across groups and may, thus, mask actual differences between groups in volume loss. Alternatively, the patient groups under study could be matched by the length of the CS, in the same manner as they are for other variables, such as age.

We pursued this issue further by empirically studying whether EC volumes were different when derived from protocols using the two methods of defining the lateral border. We found that the distributions across individuals were very similar between the two methods, and yielded a coefficient of correlation of 0.934. Such a high correlation means that in any regression analysis with other variables, the two methods of EC measurement would give essentially the same result.

We confirmed the finding that the EC volume has very high individual variability [27]. Compared to the values of individual variability (coefficients of variation of 27%–28%), our coefficients of reproducibility for the EC (which have comparable metrics) were approximately 10 times smaller (1.67–2.29% for intra-rater, and 2.38–3.37% for inter-rater reproducibility). Our data of reproducibility were lower than those reported for the EC previously [7.4%, [27]] and comparable to that reported for the HF [1.9%, [30]]. These relatively small values of the raters' disagreement compared to the larger values of individual differences within the data show that the EC was measured with a high level of reliability. The estimated level of reliability achieved in this study (0.9591–0.997) exceeded a critical value of "almost perfect" reliability at $P < 0.00001$ level of significance.

In summary, we have described a reliable method that allows the in vivo measurement of both the EC and the HF from the same oblique coronal MRI sections. The major advantage of using similarly oriented MRI slices to derive the volume of both structures is that overestimation of one of these two adjacent regions at the expense of the other is prevented. This volumetric method should provide a valuable tool for detecting and comparing atrophy of both structures in vivo in very early AD and in the incipient stages of the disease.

Acknowledgments

We thank Dr. Gary W. Van Hoesen for his generous advice in the development of this protocol.

References

[1] Amaral D, Insausti R. Hippocampal formation. In: Paxinos G, editor. The human nervous system. San Diego: Academic Press, 1990:711–55.
[2] Arriagada PV, Growdon JH, Hedley-Whyte ET, Hyman BT. Neurofibrillary tangles but not senile plaques parallel duration and severity of Alzheimer's disease. Neurology 1992;42:631–9.
[3] Barta PE, Powers RE, Aylward EH, Chase GA, Harris GJ, Rabins PV, Tune LE, Pearlson GD. Quantitative MRI volume changes in late onset schizophrenia, and Alzheimer's disease compared to normal controls. Psychiatry Res 1992;68:65–75.
[4] Bobinski M, de Leon MJ, Convit A, De Santi S, Wegiel J, Tarshish CY, Louis LAS, Wisniewski HM. MRI of entorhinal cortex in mild Alzheimer's disease. Lancet 1999;353:38–40.
[5] Braak H, Braak E. Neuropathological stageing of Alzheimer-related change. Acta Neuropathol 1991;82:239–59.
[6] Braak H, Braak, E. The human entorhinal cortex: normal morphology and lamina- specific pathology in various diseases. Neurosci Res 1992;15:6–31.
[7] Braak, H, Braak, E. Staging of Alzheimer's disease-related neurofibrillary changes. Neuorobiol Aging 1995;16:271–82.
[8] Braak H, Braak E, Yilmazer D, Bohl J. Functional anatomy of human hippocampal formation and related structures. J Child Neurol 1996; 11:265–75.
[9] Convit A, de Leon MJ, Tarshish C, De Santi S, Tsui W, Rusinek H, George A. Specific hippocampal volume reduction in individuals at risk for Alzheimer's disease. Neurobiol Aging 1997;18:131–8.
[10] Dani SU, Pittella JE, Boehme A, Schneider B. Progressive formation of neuritic plaques and neurofibrillary tangles is exponentially related to age and neuronal size. A morphometric study of three geographically distinct series of aging people. Dement Geriatr Cogn Disord 1997;8:217–27.
[11] de Leon MJ, George AE, Golomb J, Tarshish C, Convit A, Kluger A, De Santi S, McRae T, Ferris SH, Reisberg B, Ince C, Rusinek H, Bobinski M, Quinn B, Miller DC, Wisniewski HM. Frequency of hippocampal formation atrophy in normal aging and Alzheimer's disease. Neurobiol Aging 1997;18:1–11.
[12] deToledo-Morrell L, Sullivan MP, Morrell F, Wilson RS, Bennett DA, Spencer S. Alzheimer's disease: in vivo detection of differential vulnerability of brain regions. Neurobiol Aging 1997;18:463–8.
[13] deToledo-Morrell L, Dickerson B, Sullivan MP, Spanovic C, Wilson R, Bennett DA. Hemispheric differences in hippocampal volume predict verbal and spatial memory performance in patients with Alzheimer's disease. Hippocampus 2000;10:136–42.
[14] Desmond PM, O'Brien JT, Tress BM, Ames DJ, Clement JG, Clement P, Schweitzer I, Tuckwell V, Robinson GS. Volumetric and visual assessment of the mesial temporal structures in Alzheimer's disease. Austr NZ J Med 1994;24:547–53.
[15] Dickerson BC, Goncharova II, Sullivan MP, Forchetti C, Wilson RS, Bennett DA, Beckett L, deToledo-Morrell L. MRI-derived entorhinal, and hippocampal volume in incipient, and very mild Alzheimer's disease. Neurobiol Aging 2001;22:747–754.
[16] Donner A, Eliasziew M. Sample size requirements for reliability studies. Stat Med 1987;6:441–8.
[17] Duvernoy HM. The human hippocampus. New York: Springer-Verlag, 1988.
[18] Duvernoy, HM. The human brain. New York: Springer-Verlag, 1991.
[19] Ellasziew M, Young SL, Woodbury MG, Fryday-Field K. Statistical methodology for the concurrent assessment of interrater and intrarater reliability using goniometric measurements as an example. Phys Therapy 1994;74:777–88.
[20] Erkinjuntti T, Lee DH, Gao F, Steenhuis R, Eliasziw M, Fry R, Merskey, H, Hachinski VC. Temporal lobe atrophy on magnetic resonance imaging in the diagnosis of early Alzheimer's disease. Arch Neurol 1993;50:305–10.
[21] Gomez-Isla T, Price J, McKeel DW, Moris JC, Growdon JH, Hyman BT. Profound loss of layer II entorhinal cortex neurons occurs in very mild Alzheimer's disease. J Neurosci 1996;16:4491–500.
[22] Hanke J. Sulcal pattern of the anterior parahippocampal gyrus in the human adult. Anat Anz 1997;179:335–9.
[23] Heinsen H, Henn R, Eisenmenger W, Gotz M, Bohl J, Bethke B, Lockemann U, Puschel K. Quantitative investigations on the human entorhinal area: left-right asymmetry and age-related changes. Anat Embryol (Berl) 1994;190:181–94.
[24] Honeycutt NA, Smith PD, Ayward E, Li Q, Chan M, Barta PE, Pearlson GD. Mesial temporal lobe measurements on magnetic resonance imaging scans. Psychiat Res 1998;26:85–94.
[25] Hyman BT, Van Hoesen GW, Damasio AR, Barnes CL. Alzheimer's disease: cell-specific pathology isolates the hippocampal formation. Science 1984;225:1168–70.
[26] Ikeda M, Tanabe H, Nakagawa Y, Kazui H, Oi H, Yamazaki H, Harada K, Nihimura T. MRI-based quantitative assessment of the hippocampal region in very mild to moderate Alzheimer's disease. Neuroradiology 1994;36:7–10.
[27] Insausti R, Juottonen K, Soininen H, Insausti AM, Partanen K, Vainio P, Laakso MP, Pitkanen A. MR volumetric analysis of the human entorhinal, perirhinal, and temporopolar cortices. Am J Neuroradiol 1998;19:659–71.
[28] Insausti R, Tunont T, Sobreviela T, Insausti AM, Gonzalo LM. The human entorhinal cortex: a cytoarchitectonic analysis. J Comp Neurol 1995;355:171–98.
[29] Jack CR, Petersen RC, O'Brien PC, Tangalos EG. MR-based hippocampal volumetry in the diagnosis of Alzheimer's disease. Neurology 1992;42:183–8.
[30] Jack C, Petersen R, Xu YC, Waring SC, O'Brien PC, Tangalos EG, Smith GE, Ivnik RJ, Kokmen E. Medial temporal atrophy on MRI in normal aging and very mild Alzheimer's disease. Neurology 1997; 49:786–94.
[31] Juottonen K, Laakso MP, Insausti R, Lehtovirta M, Pitkanen A, Partanen K, Soininen H. Volumes of the entorhinal and perirhinal cortices in Alzheimer's disease. Neurobiol Aging 1998;19:15–22.
[32] Juottonen K, Laakso MP, Partanen K, Soininen H. Comparative MR analysis of the entorhinal cortex, and hippocampus in diagnosing Alzheimer's disease. Am J Neuroradiol 1999;20:139–44.
[33] Kaye JA, Swihart T, Howieson D, Dame A, Moore MM, Karnos T, Camicioli R, Ball M, Oken B, Sexton G. Volume loss of the hippocampus and temporal lobe in healthy elderly persons destined to develop dementia. Neurology 1997;48:1297–304.
[34] Kesslak JP, Nalcioglu O, Cotman CW. Quantification of magnetic resonance scans for hippocampal and parahippocampal atrophy in Alzheimer's disease. Neurology 1991;41:51–4.

[35] Killiany RJ, Moss MB, Albert MS, Sandor T, Tieman J, Jolesz F. Temporal lobe regions on magnetic resonance imaging identify patients with early Alzheimer's disease. Arch Neurol 1993;50:949–54.
[36] Killiany RJ, Gomez-Isla T, Moss M, Kikinis R, Sandor T, Jolesz F, Tanzi R, Jones K, Hyman BT, Albert MS. Use of structural magnetic resonance imaging to predict who will get Alzheimer's disease. Ann Neurol 2000;47:430–9.
[37] Krasuski JS, Alexander GE, Horwitz B, Daly EM, Murphy DG, Rapoport SI, Schapiro MB. Volumes of medial temporal lobe structures in patients with AD and mild cognitive impairment (and in healthy controls). Biol Psychiatry 1998;43:60–8.
[38] Krimer LS, Hyde TM, Herman MM, Saunders RC. The entorhinal cortex: an examination of cyto- and myeloarchitectonic organization in humans. Cerebral Cortex 1997;7:722–31.
[39] Laakso MP, Soininen H, Partanen K, Helkala EL, Hallikainen P, Vainio P, Hallikainen M, Hanninen T, Riekkinen PJ. Volumes of hippocampus, amygdala, and frontal lobes in the MRI-based diagnosis of early Alzheimer's disease: correlations with memory functions. J Neural Transm Park Dis Dement Sect 1995;9:73–86.
[40] Landis JR, Koch GG. The measurement of observer agreement for categorical data. Biometrics 1977;33:159–74.
[41] Lehericy S, Baulac M, Chiras J, Pierot L, Martin N, Pillon B, Deweer B, Dubois B, Marsault C. Amygdalohippocampal MR volume measurements in the early stages of Alzheimer disease. Am J Neuroradiol 1994;15:929–37.
[42] Mizutani T, Kasahara M. Hippocampal atrophy secondary to entorhinal cortical degeneration in Alzheimer-type dementia. Neurosci Let 1997;222:119–22.
[43] O'Brien JT, Desmond P, Ames D, Schweitzer I, Chiu E, Tress B. Temporal lobe magnetic resonance imaging can differentiate Alzheimer's disease from normanl ageing, depression, vascular dementia and other causes of cognitive impairment. Psychol Med 1997;27:1267–75.
[44] Parnetti L, Lowenthal DT, Presciutti O, Pelliccioli GP, Palumbo R, Gobbi G, Chiarini P, Palumbo B, Tarducci R, Senin U. 1H-MRS, MRI-based hippocampal volumetry, and 99 mTc-HMPAO-SPECT in normal aging, age-associated memory impairment, and probable Alzheimer's disease. J Am Geriatr Soc 1996;44:133–1338.
[45] Pearlson GD, Harris GJ, Powers RE, Barta PE, Camargo EE, Chase GA, Noga JT, Tune LE. Quantitative changes in mesial temporal volume, regional cerebral flow, and cognition in Alzheimer's disease. Arch Gen Psychiatr 1992;49:402–8.
[46] Shrout PE, Fleiss JL. Intraclass correlation: uses in assessing rater reliability. Psychol Bull 1979;86:420–8.
[47] Small GW, Leiter F. Neuroimaging for diagnosis of dementia. J Clin Psychiatr 1998;59(Suppl.11):4–7.
[48] Squire LR, Zola-Morgan S. The medial temporal lobe memory system. Science 1991;253:1380–6.
[49] Van Hoesen GW. Anatomy of the medial temporal lobe. Magn Res Imaging 1995;13:1047–55.
[50] Van Hoesen GW. Ventromedial temporal lobe anatomy, with comments on Alzheimer's disease and temporal injury. J Neuropsychiat Clin Neurosci 1997;9:331–41.
[51] Van Hoesen GW, Hyman BT, Damasio AR. Entorhinal cortex pathology in Alzheimer's disease. Hippocampus 1991;1:1–8.
[52] Xu Y, Jack CR, O'Brien PC, Kokmen E, Smith GE, Ivnik RJ, Boeve BF, Tangalos RG, Petersen RC. Usefulness of MRI measures of entorhinal cortex versus hippocampus in AD. Neurology 2000;54:1760–7.
[53] Young BJ, Otto T, Fox GD, Eichenbaum H. Memory representation within the parahippocampal region. J Neurosci 1997;17:5183–95.
[54] Zola-Morgan S, Squire LR, Ramus SJ. Severity of memory impairement in monkeys as a function of locus and extent of damage within the medial temporal lobe memory system. Hippocampus 1994;4:483–95.